A fluorescence-based assay for quantitative analysis of phospholipid:diacylglycerol acyltransferase activity

Lucas Falarz [1,2], Yang Xu [1], Stacy D. Singer [3], Guanqun Chen [1,2,*]

[1] *Department of Agricultural, Food and Nutritional Science, University of Alberta, Edmonton, Alberta, Canada, T6G 2P5*

[2] *Department of Biological Sciences, University of Manitoba, Winnipeg, Manitoba, Canada, R3T 2N2*

[3] *Agriculture and Agri-Food Canada, Lethbridge Research and Development Centre, Lethbridge, Alberta, Canada T1J 4B1*

*Corresponding author: Phone: +1 (780) 492-3148; Email: gc24@ualberta.ca; Fax: + 1 (780) 492-4265 (G. Chen)

Keywords: PDAT; fluorescent diacylglycerol; nitrobenzoxadiazole; triacylglycerol biosynthesis; *in vitro* assay

20 **Abbreviations**

21

22 16:0,18:1-DAG, 1-palmitoyl-2-oleoyl-*sn*-glycerol;

23 18:1,18:1-PtdCho, 1,2-dioleoyl-*sn*-glycero-3-phosphocholine;

24 16:0,[^{14}C]18:1-PtdCho, 1-palmytoil-2-[^{14}C]oleoyl-*sn*-3-glycero-phosphocholine;

25 AtPDAT1, *Arabidopsis thaliana* PDAT1;

26 BnDGAT1, *Brassica napus* DGAT1;

27 DAG, diacylglycerol;

28 DGAT, acyl-CoA:diacylglycerol acyltransferase;

29 DHA, docosahexaenoic acid;

30 LCAT, lecithin:cholesterol acyltransferase;

31 NBD, nitrobenzoxadiazole;

32 NBD-DAG, 1-palmitoyl-2-dodecanoyl-NBD-*sn*-glycero-3-glycerol;

33 NBD-PtdCho, 1-palmitoyl-2-dodecanoyl-NBD-*sn*-glycero-3-phosphocholine;

34 PtdCho, phosphatidylcholine;

35 PDAT, phospholipid:diacylglycerol acyltransferase;

36 PMT, photomultiplier tube;

37 TAG, triacylglycerol;

38 TLC, thin-layer chromatography.

39

Abstract

Phospholipid:diacylglycerol acyltransferase (PDAT) catalyzes the acyl-CoA-independent triacylglycerol (TAG) biosynthesis in plants and oleaginous microorganisms and thus is a key target in lipid research. The conventional *in vitro* PDAT activity assay involves the use of radiolabeled substrates, which, however, are expensive and demand strict regulation. In this study, a reliable fluorescence-based method using nitrobenzoxadiazole-labeled diacylglycerol (NBD-DAG) as an alternative substrate was established and subsequently used to characterize the enzyme activity and kinetics of a recombinant *Arabidopsis thaliana* PDAT1 (AtPDAT1). We also demonstrate that the highly toxic benzene used in typical PDAT assays can be substituted with diethyl ether without affecting the formation rate of NBD-TAG. Overall, this method works well with a broad range of PDAT protein content and shows linear correlation with the conventional method with radiolabeled substrates, and thus may be applicable to PDATs from various plant and microorganism species.

53 **1. Introduction**

54 Storage lipids, which comprise mainly triacylglycerols (TAGs), are biologically and economically
55 important molecules. TAG is composed of a glycerol backbone and three long-chain fatty acids, and is
56 stored in high quantities (up to 70% of the microalgal biomass and seed weight in some oilseed plants)
57 as an energy source in many organisms (Hu et al., 2008; Li-Beisson et al., 2016). Indeed, various
58 species have been examined as potential sources of vegetable oils and/or fatty acids, which can be used
59 for food, feed, biofuel and industrial purposes. For instance, docosahexaenoic acid (DHA) produced in
60 certain microalgae has important nutraceutical applications, while ricinoleic acid found in castor
61 (*Ricinus communis*) seeds is used as a feedstock for the production of high performance polymers,
62 coatings, varnishes, lubricants, cosmetics and surfactants (Dyer et al., 2008; McKeon, 2016; Mutlu &
63 Meier, 2010).

64 The formation of different TAG species is largely controlled by the substrate specificity of the
65 acyltransferases that sequentially transfer fatty acyl chains to the *sn*-1, 2, and 3 positions of a glycerol
66 backbone (Xu et al., 2018). While the first two acylation steps are catalyzed by enzymes with acyl-CoA
67 as the sole acyl donor, the final step involving the acylation of diacylglycerol (DAG) to form TAG can
68 be carried out in either acyl-CoA-dependent and acyl-CoA-independent reactions, catalyzed by acyl-
69 CoA:diacylglycerol acyltransferase (DGAT) and phospholipid:diacylglycerol acyltransferase (PDAT;
70 EC 2.3.1.158), respectively. Although DGAT (especially DGAT1) appears to be the major contributor
71 to TAG biosynthesis in oil crops, PDAT, which uses membrane phospholipids as acyl donors to acylate
72 DAG (Fig. 1; Dahlqvist et al., 2000), also makes a significant contribution and plays an important role
73 in channeling unusual fatty acids into TAG in some plant species (Dahlqvist et al., 2000; Pan et al.,
74 2013; Stahl et al., 2004; van Erp et al., 2011; Xu et al., 2018). For example, PDAT from castor bean
75 (*Ricinus communis*) and hawk's-beard (*Crepis palaestina*) preferentially incorporate ricinoleoyl and
76 vernoloyl moieties into TAG, respectively, while flax (*Linum usitatissimum*) PDAT prefers substrates
77 containing α-linolenic acid (Dahlqvist et al., 2000; Pan et al., 2013).

78 Given the important role of PDAT in TAG biosynthesis, this enzyme is increasingly being used
79 as a target for the enhancement of oil content and development of designer specialty oils enriched in
80 desirable fatty acids using genetic engineering approaches (Bates et al., 2014; Dahlqvist et al., 2000;
81 Kim et al., 2011; Pan et al., 2013; van Erp et al., 2011; van Erp et al., 2015; Xu et al., 2018). *In vitro*
82 assays of PDATs to estimate their enzymatic activities, combined with *in vivo* studies, have been
83 proven to be a powerful approach with which to characterize these valuable enzymes (Stahl et al.,
84 2004; Yoon et al., 2012). However, *in vitro* assays of PDAT activities with radiolabeled substrates is a
85 standard biochemical method, which depends on the use of expensive radiolabeled chemicals and may
86 require separate laboratory areas, strict and tedious regulation processes, and extra training of
87 personnel. Therefore, it would be advantageous to establish alternative methods for such assays that do
88 not require the use of radiolabeled chemicals (McFie & Stone, 2011; Sakurai et al., 2018).
89 Fluorescent compounds have been used to replace those that are radiolabeled in certain *in vitro*
90 enzymatic assays, including those involving DGAT, previously (Huang et al., 2018; McFie & Stone,
91 2011; Sakurai et al., 2018; Sanderson & Venable, 2012). However, the quantification of PDAT activity
92 with non-radiolabelled substrates has yet to be established. The current study describes the
93 development of a fluorescence-based *in vitro* method for the quantification of PDAT activity. Using
94 phosphatidylcholine (PtdCho) as the acyl donor and DAG labeled with nitrobenzoxadiazole (NBD) as
95 the acyl acceptor, the activity of recombinant *Arabidopsis thaliana* PDAT1 (AtPDAT1) was quantified.
96 Moreover, alternative solvents to highly toxic benzene, which is typically used in PDAT assays, were
97 also assessed. This fluorescence-based method for *in vitro* PDAT assay is safer, less costly and more
98 convenient than the one using radiolabeled chemicals, and thus will increase the feasibility of future
99 PDAT studies.
100
101 **2. Materials and Methods**
102 2.1. Genes, enzymes and chemicals

103 AtPDAT1 (AT5G13640) and *Brassica napus* DGAT1 (BnDGAT1; GenBank accession No.:
104 JN224473; used as a positive control for the production of NBD-TAG) were used in enzymatic assays.
105 The full-length *AtPDAT1* coding sequence was previously isolated in our laboratory using cDNA
106 synthesized from total RNA extracted from *A. thaliana* (Col-0) siliques as template. The *AtPDAT1*
107 coding sequence was cloned into the pYES2/NT vector (Invitrogen, Burlington, ON, Canada) for yeast
108 heterologous expression using forward primer (5'- CAG AGC GGC CGC TAT GCC CCT TAT TCA
109 TCG GAA AAA GCC GAC -3') and reverse primer (5'- GCT CTA GAT CAC AGC TTC AGG TCA
110 ATA CGC TCC GAC C - 3'). Similarly, the *BnDGAT1* coding sequence was also previously isolated
111 in our laboratory and was cloned into the pYES2.1/V5-His TOPO vector (Invitrogen; Xu et al., 2017).
112 Lipids, including the fluorescent substrate 1-palmitoyl-2-{12-[(7-nitro-2-1,3-benzoxadiazol-4-
113 yl) amino] dodecanoyl}-*sn*-glycero-3-phosphocholine (NBD-PtdCho), 1,2-dioleoyl-*sn*-glycero-3-
114 phosphocholine (18:1,18:1-PtdCho), 1-palmitoyl-2-oleoyl-*sn*-glycerol (16:0,18:1-DAG), and oleoyl-
115 CoA were purchased from Avanti Polar Lipids Inc. (Alabaster, AL, USA). 1-palmytoil-2-[^{14}C]oleoyl-
116 *sn*-3-glycero-phosphocholine (16:0,[^{14}C]18:1-PtdCho; 55 µCi/µmol) was acquired from American
117 Radiolabeled Chemicals (St. Louis, MO, USA). Phospholipase C used for the synthesis of NBD-DAG
118 was purchased from Sigma-Aldrich (Oakville, ON, Canada).
119
120 2.2. Yeast transformation
121 Constructs containing *AtPDAT1* and *BnDGAT1* were individually transformed into the *Saccharomyces*
122 *cerevisiae* H1246 strain (*MATα are1-Δ::HIS3, are2-Δ::LEU2, dga1-Δ::KanMX4, lro1-Δ::TRP1*
123 *ADE2*), which lacks the ability to synthesize TAG (Sandager et al., 2002), using the lithium
124 acetate/single-stranded carrier DNA/PEG method (Gietz & Schiestl, 2007). Briefly, *S. cerevisiae*
125 H1246 was cultivated in YPD medium (1% yeast extract, 2% peptone, 2% dextrose) at 30ºC with
126 shaking at 220 rpm for 24 h. Subsequently, 2 ml of the yeast culture was used to inoculate 50 ml of
127 YPD medium and the yeast culture was grown at 30ºC with shaking at 220 rpm until the cell

128 concentration reached an OD_{600} of 0.6 - 0.8. Yeast cells were then harvested by centrifugation at 3,000
129 g for 3 min, washed twice with sterile water and once with LiTE solution (100 mM lithium acetate, 10
130 mM Tris, 1 mM EDTA, pH 7.5). Yeast cells were subsequently resuspended in 1ml of LiTE solution.
131 For yeast transformation, 100 µl of the resuspended yeast cells were mixed with 5 µl of 2 µg/µl
132 deoxyribonucleic acid sodium salt from salmon testes (Sigma-Aldrich), 500 µl 40% PEG3350-LiTE
133 solution (40% PEG 3350, 100 mM lithium acetate, 10 mM Tris, 1 mM EDTA), 60 µl of DMSO, and
134 600 ng of the plasmid containing *AtPDAT1* or *BnDGAT1* coding sequences. The mixtures were
135 incubated at room temperature for 15 min, followed by heat shock at 42ºC for 15 min. The yeast cells
136 were then spread on agar plates composed of solid minimal media lacking uracil [0.67% yeast nitrogen
137 base, 0.2% synthetic complete medium lacking uracil (SC-Ura), 2% dextrose, and 2% (w/v) agar] and
138 incubated at 30ºC. Transformants were identified as colonies that grew in the absence of uracil. A yeast
139 strain containing *Lac*Z developed in our laboratory previously was used as a negative control in
140 enzymatic assays (Xu et al., 2018).
141
142 2.3. Yeast cultivation and microsomal preparation
143 Yeast cultivation and microsomal preparation were carried out using a previously described method
144 with slight modifications (Xu et al., 2018). Briefly, *S. cerevisiae* H1246 strains hosting *AtPDAT1,*
145 *BnDGAT1* or *LacZ* were first grown in liquid minimal media lacking uracil (0.67% yeast nitrogen base,
146 0.2 % SC-Ura and 2% raffinose) at 30ºC with shaking at 220 rpm for 24 h. These yeast cells were then
147 used to inoculate induction media (liquid minimal media containing 2% galactose and 1% raffinose) to
148 an initial OD_{600} of 0.2. Cultures were then grown under the same conditions until the OD_{600} reached
149 approximately 6.0. Yeast cells were harvested by centrifugation at 3,000 g for 5 min, washed once with
150 distilled water, and resuspended in a lysis buffer containing 20 mM Tris-HCl (pH 7.9), 2 mM
151 dithiothreitol, 10 mM magnesium chloride, 1mM EDTA, 5% glycerol (by volume), and 300 mM
152 ammonium sulfate. Harvested yeast cells were disrupted through homogenization with 0.5 mm glass

153 beads in a bead beater (Biospec, Bartlesville, OK, USA), followed by centrifugation at 10,000 *g* for 20
154 min. The supernatant was subsequently recovered and centrifuged at 100,000 *g* for 70 min, and the
155 resulting pellet (microsomal fraction) was resuspended in 0.1M potassium phosphate buffer (pH 7.2).
156 Protein concentration was measured using the Bradford method with bovine serum albumin as the
157 standard (Bradford, 1976). All steps were performed at 4ºC.
158
159 2.4. Synthesis of NBD-DAG
160 NBD-DAG was synthesized from NBD-PtdCho in a reaction catalyzed by phospholipase C as
161 described previously (Sanderson & Venable, 2012). In brief, 1 mg of NBD-PtdCho was dissolved in
162 500 µl of a diethyl ether/ethanol mixture (98:2, by volume) in a screw cap culture tube. Subsequently,
163 15 µl of 0.02 M calcium chloride and 20 µl of phospholipase C (1 unit) were added to the glass tube.
164 The mixture was then incubated at room temperature with agitation for 2 h. Following the reaction,
165 lipids in the mixture were extracted using the Bligh and Dyer method (Bligh & Dyer, 1959), dried
166 under nitrogen gas, resuspended in 100 µl of chloroform/methanol (2:1, by volume) and spotted on a
167 pre-coated thin-layer chromatography (TLC) plate (SIL G-25, Macherey-Nagel, Düren, Germany). The
168 TLC plate was developed in hexane/diethyl ether/methanol/acetic acid (70:30:5:1, by volume). The
169 NBD-DAG band was visualized under UV light, scraped, and transferred to a screw cap culture tube.
170 The synthesized NBD-DAG was extracted using the Bligh and Dyer method, dissolved in chloroform,
171 purged with nitrogen and stored at -20ºC for further use.
172
173 2.5. *In vitro* DGAT assays
174 *In vitro* DGAT assays (used as a positive control for the production of NBD-TAG) were carried out
175 using microsomes containing recombinant BnDGAT1, along with NBD-DAG and oleoyl-CoA as
176 substrates as described previously with slight modifications (Sanderson & Venable, 2012; Xu et al.,
177 2017). Briefly, reaction mixtures (50 µl) were composed of 238 mM HEPES-NaOH (pH 7.4), 3.85 mM

178 $MgCl_2$, 400 μM NBD-DAG, 0.02% Tween 20 (by volume), 18 μM oleoyl-CoA and 10 μl of
179 microsomes containing BnDGAT1 or LacZ (negative control). Reactions were initiated through the
180 addition of the yeast microsomes, and were incubated at 30ºC for 60 min, followed by quenching with
181 100 μl of chloroform/methanol (2:1, by volume). All reactions (and hereafter) were performed in
182 triplicate.
183
184 2.6. *In vitro* PDAT assays
185 Unless otherwise indicated, PDAT assays were conducted as described previously (Dahlqvist et al.,
186 2000), except that NBD-DAG and unlabeled PtdCho were used in place of unlabeled DAG and
187 radiolabeled PtdCho as the acyl acceptor and acyl donor, respectively. Yeast microsomes containing 40
188 μg of protein were aliquoted to reaction tubes, flash-frozen in liquid nitrogen and freeze-dried
189 overnight. Subsequently, 1.5 nmol of NBD-DAG and 2.5 nmol of 18:1,18:1-PtdCho dissolved in 14 μl
190 of benzene were added to the microsomes. The benzene was immediately evaporated under a stream of
191 N_2 to avoid loss of enzymatic activity. The reaction was then initiated by adding 100 μl of 50 mM
192 potassium phosphate buffer (pH 7.2). The reaction mix, which had 15 μM of NBD-DAG and 25 μM of
193 18:1,18:1-PtdCho, was incubated at 30ºC for 60 min, followed by quenching with 100 μl of
194 chloroform/methanol (2:1, by volume).
195 For the determination of the time course of NBD-TAG production, samples were collected from
196 0 to 120 min. To verify the effects of yeast microsome amount in the assay, the equivalent of 0-240 μg
197 of protein was individually used in the assays. To measure the enzymatic kinetics of AtPDAT1,
198 different NBD-DAG concentrations in the range of 10 to 60 μM were used in the reactions. In order to
199 validate the fluorescence-based assay, we also carried out the conventional PDAT assay using
200 radiolabeled chemicals and a wide range of microsomal protein contents containing recombinant
201 AtPDAT1 (0, 20, 40, and 80 μg of protein). In the conventional radioisotope-based PDAT assay, 1.5
202 nmol of 16:0,18:1-DAG and 2.5 nmol of 16:0,[^{14}C]18:1-PtdCho (equivalent of 15 μM of DAG and 25

203 μM of PtdCho in the final mixture) were dissolved in 14 μl of benzene to be added in the dried
204 microsomes. In the experiment to identify the ideal alternative solvent to benzene, 14 μl of diethyl ether
205 or ethanol were used to dissolve the substrates and all other parameters were kept the same.
206
207 2.7. Visualization of products formed in PDAT and DGAT assays
208 To separate the products formed in PDAT and DGAT assays with fluorescent chemicals, the
209 chloroform phases (lipid fractions) of quenched reaction mixtures were spotted on TLC plates, which
210 were then developed in diethyl ether/hexane/methanol/acetic acid (60:40:5:1, by volume). The TLC
211 plates were then dried and 10 μl of NBD-PtdCho (0.01 mg/ml) was spotted at the top of each plate as
212 an internal standard. The fluorescence of each spot was used for visualization purposes by scanning
213 TLC plates in a Typhoon FLA 9500 (GE Healthcare, Mississauga, ON, Canada) with excitation and
214 emission wavelengths of 495 nm and 519 nm, respectively. The photomultiplier tube (PMT) voltage
215 was set to 250 V. In terms of the conventional PDAT assay using radiolabeled chemicals, the products
216 of the enzymatic reactions were separated on TLC plates developed with hexane/diethyl ether/acetic
217 acid (80:20:1.5, by volume). The radiolabelled TAG formed was located with phosphorimaging in the
218 Typhoon FLA 9500 and quantified in a Beckman-Coulter LS6000.
219
220 2.8. Generation of a standard curve and quantification of NBD-TAG
221 A standard curve of NBD fluorescent intensity versus the amount of lipids was established as described
222 previously (Sanderson & Venable, 2012). In brief, 10 μl aliquots of a dilution series of NBD-DAG (in
223 the range of 0.5 pmol to 220 pmol) were loaded on TLC plates in triplicate. Fluorescence was detected
224 on a Typhoon FLA 9500 as described above, and the intensity of each spot was quantified using
225 ImageJ 1.52a (Schneider et al., 2012). The intensity of fluorescence was then plotted against the
226 amount of NBD-DAG, and the standard curve was generated by linear regression. To quantify NBD-

227 TAG, fluorescent intensity was normalized using the NBD-PtdCho internal standard, and background
228 fluorescence was subtracted from the total reading of the NBD-TAG band.
229
230 2.9. Statistical analyses
231 Plots and statistical analyses were carried out with GraphPad Prism 8. Error bars represent the standard
232 deviation of the results. Student's *t*-test was employed to compare the effects of different solvents in
233 the PDAT assay.
234
235
236 **3. Results and Discussion**
237 3.1. Establishment of a PDAT assay with NBD-labelled substrate
238 In previous studies, PDAT assays have been conducted using phospholipids with a radiolabeled acyl
239 chain at the *sn*-2 position and regular DAG as substrates (Dahlqvist et al., 2000; Stahl et al., 2004). To
240 avoid the use of radioactive chemicals, we examined the effectiveness of a fluorescence-based method
241 for assessing PDAT activity. The use of fluorescent substrates has also been estimated to reduce the
242 cost of DGAT assays by 75% (McFie & Stone, 2011), which would provide another benefit to the
243 development of a fluorescence-based PDAT assay. Lipids containing an NBD fluorescent group were
244 chosen for the establishment of this assay since NBD has been successfully used previously in *in vitro*
245 assays of other lipid biosynthetic enzymes, such as DGAT (McFie & Stone, 2011; Sanderson &
246 Venable, 2012).
247 On the commercial NBD-PtdCho, the relatively big NBD molecular group is linked to the end
248 of the acyl chain at the *sn*-2 position, which is transferred to the *sn*-3 position of DAG in the PDAT
249 reaction. To minimize the potential effects of the NBD molecular structure on PDAT assay, NBD-DAG
250 and regular PtdCho were used in this study. Since NBD-DAG is not commercially available, this

251 compound was synthesized from NBD-PtdCho. This synthesized NBD-DAG contains a palmitoyl
252 chain at the *sn*-1 position and an NBD molecule linked to a dodecanoyl chain at the *sn*-2 position.
253 Similar to NBD-DAG, NBD-TAG, which is required to confirm the success of the PDAT
254 reaction with NBD-DAG as substrate, is also not commercially available. To overcome this,
255 recombinant BnDGAT1 was used to convert NBD-DAG to NBD-TAG. As shown in Fig. 2, NBD-
256 TAG synthesized by BnDGAT1, which has been validated in the DGAT1 reaction, has the same
257 migration distance as the product of recombinant AtPDAT1 on a TLC plate, confirming that the
258 product of AtPDAT1 was indeed an NBD-TAG molecule. This result suggests that NBD-DAG can be
259 used as a substrate by PDAT for catalysis. Since the substrate binding-pocket of lysosomal
260 phospholipase A_2, a homolog to PDAT, has been found to have a higher conformational flexibility to
261 accept different substrates (Glukhova et al., 2015), PDAT may have similar flexible regions that are
262 able to accept NBD-DAG.
263 In order to quantify NBD-TAG produced in PDAT assays, a standard curve was generated
264 based on the fluorescence of known quantities of NBD-DAG (Fig. 3). When different dilutions of
265 NBD-DAG (0.5 - 220 pmol) were spotted on a TLC plate, the lowest detectable amount of NBD-DAG
266 was 0.5 pmol (Fig. 3a). This detection limit is similar to that (0.1 pmol) reported in a previous study
267 (Sanderson & Venable, 2012), even though they worked with different fluorescence scanners and PMT
268 voltage (250 V in the present study versus 420 V in the other study). In any case, the production of
269 NBD-TAG by AtPDAT1 was substantially higher than 0.5 pmol in the enzymatic assay, and therefore
270 the detection limit observed here was sufficiently sensitive for our purposes.
271 When fluorescence intensity was plotted against the amount of NBD-DAG, a standard curve
272 was obtained by linear regression of the linear region from 0.5 pmol to 80 pmol of NBD-DAG (Fig.
273 3b). The amount (pmol) of NBD-TAG produced in PDAT reactions could then be quantified using the
274 equation *NBD-TAG = 0.01519 x corrected fluorescence intensity* (R^2=0.979).
275

276 3.2. Characterization of AtPDAT1 using a fluorescence-based PDAT assay

277 After confirming that a fluorescence-based method was suitable for *in vitro* PDAT assays, we further
278 investigated if this method would be suitable for the characterization of AtPDAT1. The time course of
279 the enzymatic assay indicated that the formation of NBD-TAG could increase in a linear fashion up to
280 a maximum of 60 min of reaction time (Fig. 4; $R^2 = 0.995$). Unexpectedly, the microsomes of *S.*
281 *cerevisiae* H1246 expressing *LacZ* produced very low amounts of an unknown fluorescent compound
282 with a similar migration distance to NBD-TAG on TLC plates (Fig. 4), but PDAT reactions using
283 boiled microsomes as the enzyme source did not (Fig. 5), which suggests the presence of an unknown
284 but very weak enzymatic reaction in our *LacZ* negative control microsomes. Since *S. cerevisiae* H1246
285 is a quadruple mutant that lacks all genes necessary for neutral lipid biosynthesis (*DGA1*, *LRO1*, *ARE1*,
286 and *ARE2*; Sandager et al., 2002), the resulting bands in the negative control microsomal samples were
287 unlikely due to any presence of PDAT or TAG. These fluorescence signals generated in the negative
288 control samples were thus treated as a background signal and subtracted from the fluorescence signals
289 generated by the recombinant AtPDAT1.

290 The effects of protein content on PDAT activity was also subsequently analyzed. As shown in
291 Fig. 6, the NBD-TAG formation increased in a linear fashion up to a maximum of 80 μg of microsomal
292 protein ($R^2 = 0.974$). The biosynthesis of fluorescent TAG did not increase any further with higher
293 enzyme amounts, which was likely due to a limitation of available substrates. This result is consistent
294 with a previous study involving a fluorescence-based assay of DGAT activity, where a protein content
295 above 50 μg did not yield any further increases in NBD-TAG production (McFie & Stone, 2011). In
296 addition, there was a good correlation ($R^2 = 0.919$) between the fluorescence-based PDAT assay and
297 the conventional assay that was carried out with 16:0,[^{14}C]18:1-PtdCho and 16:0,18:1-DAG as the
298 substrates (Fig. 7).

299 The enzyme kinetics of AtPDAT1 in response to different concentrations of NBD-DAG were
300 also assessed. As shown in Fig. 8, AtPDAT1 displayed a Michaelis-Menten response to an increasing

301 concentration of NDB-DAG with apparent V_{max} and K_m values of 11.1 pmol NBD-TAG/min/mg
302 protein and 32.6 μM, respectively. The data obtained with the conventional assay for AtPDAT1 also
303 followed Michaelis-Menten kinetics with respect to 16:0,18:1-DAG with apparent V_{max} and K_m values
304 of 2.0 pmol NBD-TAG/min/mg protein and 39.5 μM, respectively. Similarly, lecithin:cholesterol
305 acyltransferase (LCAT), which belongs to the same family as PDAT, also shows Michaelis-Menten
306 kinetics (Pan et al., 2015; Sakurai et al., 2018). It should be noted that the obtained apparent K_m values
307 of AtPDAT1 from the conventional and the fluorescence-based methods are close, whereas the
308 apparent V_{max} values from both methods differ largely. The difference in the apparent V_{max} values from
309 both methods is likely caused by the usage of different labeled substrates ([^{14}C] PtdCho or NBD-DAG).
310 Since yeast microsomes contain a substantial amount of PtdCho, the added [^{14}C] PtdCho in the
311 conventional PDAT reaction system was diluted by the bulk membrane phospholipids, which leads to
312 underestimation of the formed [^{14}C] TAG and thus a lower calculated value of enzyme activity than the
313 real one. The apparent kinetic parameters of AtPDAT1 obtained with different assay methods may also
314 be affected by the properties of different PtdCho (16:0,[^{14}C]18:1-PtdCho vs 18:1,18:1-PtdCho) and
315 DAG (16:0,18:1-DAG vs NBD-DAG) molecules used in the assays. When using microsomal fractions
316 as the enzyme source to assay the activity of membrane-bound PtdCho metabolic enzymes, such as
317 PDAT, the enzyme reaction rate is typically controlled by the accessibility of enzyme to the exogenous
318 substrates. A more polar substrate such as NBD-DAG may be easier to be diffused across the
319 endogenous membrane lipids during the benzene mediated substrate deliver process and reach the close
320 proximity to the enzyme for catalysis. In the future, it would be interesting to use purified PDAT for
321 kinetic studies where the accessibility of enzyme to the substrates is not potentially affected by the
322 microsomal lipids, leading to a less complex kinetic situation.
323
324 3.3. Substitution of benzene in PDAT assays

325 Benzene is used in PDAT assays to dissolve and deliver substrates to the microsomal fractions. After
326 being added to the reaction tube, benzene must be immediately evaporated to prevent loss of protein
327 activity. Although benzene works well in PDAT assays, this solvent is highly hazardous. As a known
328 carcinogenic substance, benzene is also harmful to renal, cardiovascular, respiratory, and reproductive
329 systems (Bahadar et al., 2014). Even with safety measures such as fumehoods and special gloves to
330 avoid or minimize exposure to this compound, benzene poses a risk to the health of laboratory workers.
331 In order to identify an alternative solvent, diethyl ether and ethanol were tested as substitutes in our
332 PDAT assays, with all other conditions remaining the same. As shown in Fig. 9, the formation of NBD-
333 TAG with diethyl ether as the solvent was statistically equivalent to results obtained using benzene,
334 whereas NBD-TAG production was significantly lower with ethanol than with benzene as the solvent.
335 Diethyl ether was used as a safe anesthetic for medical purposes for many years though it has some
336 undesirable side effects such as post-anesthetic nausea and vomiting (Bovill, 2008). Therefore, this
337 low-toxic solvent can provide an excellent substitution for carcinogenic benzene in PDAT assays.
338

339 **4. Conclusions**

340 In summary, a fluorescence-based assay for the quantitative analysis of PDAT activity was established
341 in this study, which works well with a broad range of microsomal protein contents and reaction times,
342 and thus should provide a means to assay the activity of PDATs. Our results demonstrated that NBD-
343 DAG is a suitable substrate for *in vitro* assays of PDATs, especially for the identification of PDAT
344 activity, which is a safer, less costly and more convenient alternative to radioactive chemicals, despite
345 that the non-natural structure of the NBD-DAG may restrict the test of PDAT selectivity towards
346 different DAG molecular species. The fluorescence-based and the conventional PDAT assays have a
347 good correlation, which validates the fluorescence-based method. We also showed that the highly toxic
348 solvent benzene could be substituted with the low-toxic diethyl ether without affecting the formation
349 rate of NBD-TAG. In addition, this fluorescence-based PDAT method also set up the foundation for

350 further adaptation and development for various research purposes, such as comparing various
351 substrates, using different NBD-labelled chemicals, and combining with HPLC to develop a robust
352 medium throughput protocol for PDAT assay. Although the use of microsomal fractions in the current
353 experiment has restrictions in testing PDAT acyl specificity of PtdCho due to the influence of
354 endogenous microsomal phospholipids, this method could be further improved to test acyl specificity
355 using purified PDAT.
356

357 **Acknowledgments**

358 The authors sincerely thank Dr. Sten Stymne of Swedish University of Agricultural Sciences for
359 valuable discussions and suggestions and the yeast H1246 strain. The authors are grateful for the
360 support provided by the University of Alberta Start-up Research Grant, Alberta Innovates, Alberta
361 Agriculture and Forestry, Natural Sciences and Engineering Research Council of Canada Discovery
362 Grant (RGPIN-2016-05926), the Canada Research Chairs Program, and the University of Manitoba
363 Graduate Enhancement of Tri-Council Stipends (GETS) program.
364

365 **Conflict of interest**

366 The authors declare no conflict of interest.
367
368

369 **References**

370 Bahadar, H., Mostafalou, S., & Abdollahi, M. (2014) Current understandings and perspectives on non-
371 cancer health effects of benzene: A global concern. *Toxicology and Applied Pharmacology*,
372 **276**:83–94. https://doi.org/10.1016/j.taap.2014.02.012

373 Bates, P. D., Johnson, S. R., Cao, X., Li, J., Nam, J.-W., Jaworski, J. G., … Browse, J. (2014) Fatty
374 acid synthesis is inhibited by inefficient utilization of unusual fatty acids for glycerolipid
375 assembly. *Proceedings of the National Academy of Sciences*, **111**:1204–1209.
376 https://doi.org/10.1073/pnas.1318511111

377 Bligh, E. G., & Dyer, W. J. (1959) A rapid method of total lipid extraction and purification. *Canadian*
378 *Journal of Biochemistry and Physiology*, **37**:911–917. https://doi.org/10.1139/o59-099

379 Bovill, J. G. (2008) Inhalation anaesthesia: From diethyl ether to xenon. In J. Schüttler & H. Schwilden
380 (Eds.), *Modern anesthetics* (pp. 121–142). Berlin, Heidelberg: Springer Berlin Heidelberg.
381 https://doi.org/10.1007/978-3-540-74806-9_6

382 Bradford, M. M. (1976) A rapid and sensitive method for the quantitation of microgram quantities of
383 protein utilizing the principle of protein-dye binding. *Analytical Biochemistry*, **72**:248–254.
384 https://doi.org/10.1016/0003-2697(76)90527-3

385 Dahlqvist, A., Stahl, U., Lenman, M., Banas, A., Lee, M., Sandager, L., … Stymne, S. (2000)
386 Phospholipid:diacylglycerol acyltransferase: An enzyme that catalyzes the acyl-CoA-independent
387 formation of triacylglycerol in yeast and plants. *Proceedings of the National Academy of Sciences*,
388 **97**:6487–6492. https://doi.org/10.1073/pnas.120067297

389 Dyer, J. M., Stymne, S., Green, A. G., & Carlsson, A. S. (2008) High-value oils from plants. *Plant*
390 *Journal*, **54**:640–655. https://doi.org/10.1111/j.1365-313X.2008.03430.x

391 Gietz, R. D., & Schiestl, R. H. (2007) High-efficiency yeast transformation using the LiAc/SS carrier
392 DNA/PEG method. *Nature Protocols*, **2**:31–34. https://doi.org/10.1038/nprot.2007.13

393 Glukhova, A., Hinkovska-Galcheva, V., Kelly, R., Abe, A., Shayman, J. A., & Tesmer, J. J. (2015)
394 Structure and function of lysosomal phospholipase A2 and lecithin:cholesterol acyltransferase.
395 *Nature Communications*, **6**:6250. https://doi.org/10.1038/ncomms7250

396 Hu, Q., Sommerfeld, M., Jarvis, E., Ghirardi, M., Posewitz, M., Seibert, M., & Darzins, A. (2008)
397 Microalgal triacylglycerols as feedstocks for biofuel production: Perspectives and advances. *Plant*
398 *Journal*, **54**:621–639. https://doi.org/10.1111/j.1365-313X.2008.03492.x

399 Huang, W., Wang, X., Endo-Streeter, S., Barrett, M., Waybright, J., Wohlfeld, C., … Zhang, Q. (2018)
400 A membrane-associated, fluorogenic reporter for mammalian phospholipase C isozymes. *Journal*
401 *of Biological Chemistry*, **293**:1728–1735. https://doi.org/10.1074/jbc.RA117.000926

402 Kim, H. U., Lee, K. R., Go, Y. S., Jung, J. H., Suh, M. C., & Kim, J. B. (2011) Endoplasmic reticulum-
403 located PDAT1-2 from castor bean enhances hydroxy fatty acid accumulation in transgenic plants.
404 *Plant and Cell Physiology*, **52**:983–993. https://doi.org/10.1093/pcp/pcr051

405 Li-Beisson, Y., Nakamura, Y., & Harwood, J. (2016) Lipids: From chemical structures, biosynthesis,
406 and analyses to industrial applications. In Y. Nakamura & Y. Li-Beisson (Eds.), *Lipids in plant*
407 *and algae development* (pp. 1–18). Cham: Springer International Publishing.
408 https://doi.org/10.1007/978-3-319-25979-6_1

409 McFie, P. J., & Stone, S. J. (2011) A fluorescent assay to quantitatively measure in vitro acyl
410 CoA:diacylglycerol acyltransferase activity. *Journal of Lipid Research*, **52**:1760–1764.
411 https://doi.org/10.1194/jlr.D016626

412 McKeon, T. A. (2016) Castor (*Ricinus communis* L.). In T. A. McKeon, D. G. Hayes, D. F.
413 Hildebrand, & R. J. Weselake (Eds.), *Industrial oil crops* (pp. 75–112). New York/Urbana:
414 Elsevier/AOCS Press. https://doi.org/10.1016/B978-1-893997-98-1.00004-X

415 Mutlu, H., & Meier, M. A. R. (2010). Castor oil as a renewable resource for the chemical industry.
416 *European Journal of Lipid Science and Technology*, **112**:10–30.
417 https://doi.org/10.1002/ejlt.200900138

418 Pan, X., Peng, F. Y., & Weselake, R. J. (2015) Genome-wide analysis of
419 *PHOSPHOLIPID:DIACYLGLYCEROL ACYLTRANSFERASE* (*PDAT*) genes in plants reveals the
420 eudicot-wide *PDAT* gene expansion and altered selective pressures acting on the core eudicot
421 *PDAT* paralogs. *Plant Physiology*, **167**:887–904. https://doi.org/10.1104/pp.114.253658

422 Pan, X., Siloto, R. M. P., Wickramarathna, A. D., Mietkiewska, E., & Weselake, R. J. (2013)
423 Identification of a pair of phospholipid:diacylglycerol acyltransferases from developing flax
424 (*Linum usitatissimum* L.) seed catalyzing the selective production of trilinolenin. *Journal of*
425 *Biological Chemistry*, **288**:24173–24188. https://doi.org/10.1074/jbc.M113.475699

426 Piper, D. E., Romanow, W. G., Gunawardane, R. N., Fordstrom, P., Masterman, S., Pan, O., …
427 Walker, N. P. C. (2015) The high-resolution crystal structure of human LCAT. *Journal of Lipid*
428 *Research*, **56**:1711–1719. https://doi.org/10.1194/jlr.M059873

429 Sakurai, T., Sakurai, A., Vaisman, B. L., Nishida, T., Neufeld, E. B., Demosky, S. J., … Remaley, A.
430 T. (2018) Development of a novel fluorescent activity assay for lecithin:cholesterol
431 acyltransferase. *Annals of Clinical Biochemistry*, **55**:414–421.
432 https://doi.org/10.1177/0004563217733285

433 Sandager, L., Gustavsson, M. H., Ståhl, U., Dahlqvist, A., Wiberg, E., Banas, A., … Stymne, S. (2002)
434 Storage lipid synthesis is non-essential in yeast. *Journal of Biological Chemistry*, **277**:6478–6482.
435 https://doi.org/10.1074/jbc.M109109200

436 Sanderson, M. C., & Venable, M. E. (2012) A novel assay of acyl-CoA:Diacylglycerol acyltransferase
437 activity utilizing fluorescent substrate. *Journal of Phycology*, **48**:580–584.
438 https://doi.org/10.1111/j.1529-8817.2012.01137.x

439 Schneider, C. A., Rasband, W. S., & Eliceiri, K. W. (2012) NIH Image to ImageJ: 25 years of image
440 analysis. *Nature Methods*, **9**:671–675. https://doi.org/10.1038/nmeth.2089

441 Stahl, U., Carlsson, A. S., Lenman, M., Dahlqvist, A., Huang, B., Banás, W., … Stymne, S. (2004)
442 Cloning and functional characterization of a phospholipid:diacylglycerol acyltransferase from
443 Arabidopsis. *Plant Physiology*, **135**:1324–1335. https://doi.org/10.1104/pp.104.044354

444 van Erp, H., Bates, P. D., Burgal, J., Shockey, J., & Browse, J. (2011) Castor
445 phospholipid:diacylglycerol acyltransferase facilitates efficient metabolism of hydroxy fatty acids
446 in transgenic Arabidopsis. *Plant Physiology*, **155**:683–693. https://doi.org/10.1104/pp.110.167239

447 van Erp, H., Shockey, J., Zhang, M., Adhikari, N. D., & Browse, J. (2015) Reducing Isozyme
448 Competition Increases Target Fatty Acid Accumulation in Seed Triacylglycerols of Transgenic
449 Arabidopsis. *Plant Physiology*, **168**:36–46. https://doi.org/10.1104/pp.114.254110

450 Xu, Y., Caldo, K. M. P., Pal-Nath, D., Ozga, J., Lemieux, M. J., Weselake, R. J., & Chen, G. (2018)
451 Properties and biotechnological applications of acyl-CoA:diacylglycerol acyltransferase and
452 phospholipid:diacylglycerol acyltransferase from terrestrial plants and microalgae. *Lipids*, **53**:663–
453 688. https://doi.org/10.1002/lipd.12081

454 Xu, Y., Chen, G., Greer, M. S., Caldo, K. M. P., Ramakrishnan, G., Shah, S., … Weselake, R. J. (2017)
455 Multiple mechanisms contribute to increased neutral lipid accumulation in yeast producing
456 recombinant variants of plant diacylglycerol acyltransferase 1. *Journal of Biological Chemistry*,
457 **292**:17819–17831. https://doi.org/10.1074/jbc.M117.811489

458 Xu, Y., Holic, R., Li, D., Pan, X., Mietkiewska, E., Chen, G., … Weselake, R. J. (2018) Substrate
459 preferences of long-chain acyl-CoA synthetase and diacylglycerol acyltransferase contribute to
460 enrichment of flax seed oil with α-linolenic acid. *Biochemical Journal*, **475**:1473–1489.
461 https://doi.org/10.1042/BCJ20170910

462 Yoon, K., Han, D., Li, Y., Sommerfeld, M., & Hu, Q. (2012) Phospholipid:diacylglycerol
463 acyltransferase is a multifunctional enzyme involved in membrane lipid turnover and degradation

464 while synthesizing triacylglycerol in the unicellular green microalga *Chlamydomonas reinhardtii*.

465 *The Plant Cell*, ***24***:3708–3724. https://doi.org/10.1105/tpc.112.100701

466

467 **Figure legends**

468

469 **Fig. 1** Schematic representation of the enzymatic reaction catalyzed by phospholipid:diacylglycerol
470 acyltransferase (PDAT). PDAT catalyzes the transfer of an acyl chain from the *sn*-2 position of
471 phospholipid to the *sn*-3 position of DAG. PL, phospholipid; DAG, diacylglycerol; LPL,
472 lysophospholipid; TAG, triacylglycerol; FA, fatty acid

473

474 **Fig. 2** A representative TLC plate displaying results of enzymatic assays using fluorescence-labeled
475 substrate. Microsomal preparations from the *S. cerevisiae* quadruple mutant H1246 transformed with
476 either AtPDAT1 and BnDGAT1 were used as enzymes in the PDAT and DGAT assays, respectively.
477 For DGAT assay, fluorescent 1-palmitoyl-2-dodecanoyl-NBD-*sn*-glycero-3-glycerol (NBD-DAG) and
478 oleoyl-CoA were used as substrates. NBD-DAG spots are composed of 1,2-NBD-DAG (lower band)
479 and 1,3-NBD-DAG (upper band). Microsomes derived from yeast cells transformed with the *LacZ*
480 gene were used as the negative control. Following enzymatic assays, lipid fractions were extracted and
481 separated on TLC plates. NBD-TAG, NBD-labeled triacylglycerol. AtPDAT1, *Arabidopsis thaliana*
482 phospholipid:diacylglycerol acyltransferase 1; BnDGAT1, *Brassica napus* acyl-CoA:diacylglycerol
483 acyltransferase 1

484

485 **Fig. 3** Establishment of a standard curve for the quantification of phospholipid:diacylglycerol
486 acyltransferase (PDAT) activity. (A) Scanned image of a representative TLC plate showing the
487 fluorescence intensity of 1-palmitoyl-2-dodecanoyl-NBD-*sn*-glycero-3-glycerol (NBD-DAG) in a
488 series of molar concentrations. (B) Standard curve for the quantification of NBD-labeled molecular
489 NBD-DAG or NBD-triacylglycerol (NBD-TAG). The linear range varies from 0.5 pmol to 80 pmol of
490 NBD-DAG.

491

492 **Fig. 4** Time course curve of PDAT enzymatic reactions. Nitrobenzoxadiazole-labeled triacylglycerol
493 (NBD-TAG) produced from NBD-diacylglycerol (NBD-DAG) over time in the presence of
494 microsomal fractions from yeast heterologously expressing *Arabidopsis thaliana*
495 phospholipid:diacylglycerol acyltransferase 1 (AtPDAT1). Microsomes derived from yeast cells
496 transformed with the *LacZ* gene were used as a negative control. The reactions were catalyzed using 40
497 µg of microsomal protein in each case. All reactions were carried out with 1.5 nmol NBD-DAG, 2.5
498 nmol 18:1,18:1-PtdCho, 100 µl of phosphate buffer (pH 7.2) at 30ºC. NBD-TAG production increases
499 linearly up to 60 min (R^2 = 0.995). Values represent mean ± standard deviation (n = 3).
500
501 **Fig. 5** Production of unknown product with a similar migration distance to nitrobenzoxadiazole-labeled
502 triacylglycerol (NBD-TAG). The compound is not present in the boiled microsomal fractions from
503 yeast transformed with *LacZ*, which suggests an enzyme-catalyzed reaction. The reactions were carried
504 out using 40 µg of microsomal protein in each case. All reactions were added 1.5 nmol NBD-DAG, 2.5
505 nmol 18:1,18:1-PtdCho, and 100 µl of phosphate buffer (pH 7.2) and incubated at 30ºC for 60 min.
506
507 **Fig. 6** Production of nitrobenzoxadiazole-labeled triacylglycerol (NBD-TAG) in an enzymatic reaction
508 catalyzed by *Arabidopsis thaliana* phospholipid:diacylglycerol acyltransferase 1 (AtPDAT1) at
509 different concentrations. Microsomes derived from yeast cells transformed with the *LacZ* gene were
510 used as the negative control and weak fluorescent signals generated were subtracted from the
511 corresponding AtPDAT1 reactions as background. Microsome protein contents varied from 0 to 240 µg
512 in the reactions. All reactions were carried out with 1.5 nmol NBD-DAG, 2.5 nmol 18:1,18:1-PtdCho,
513 100 µl of phosphate buffer (pH 7.2) at 30ºC for 60 min. Values represent mean ± standard deviation (n
514 = 3).
515

516 **Fig. 7** Comparison between the fluorescence-based PDAT assay and the conventional assay with
517 radiolabeled chemicals for a wide range of microsomal protein amounts (0, 20, 40, and 80 μg)
518 containing *Arabidopsis thaliana* phospholipid:diacylglycerol acyltransferase 1 (AtPDAT1) shows a
519 good correlation (R^2 = 0.919). To avoid the influence of endogenous PtdCho on the conventional assay,
520 the amount of protein was kept constant at 80 μg by mixing microsomes derived from yeast cells
521 transformed with the *AtPDAT1* and *LacZ* genes. The conventional assay reactions were carried out with
522 2.5 nmol 16:0,[^{14}C]18:1-PtdCho, 1.5 nmol 16:0,18:1-DAG, 100 μl of phosphate buffer (pH 7.2) at 30ºC
523 for 60min. Values represent mean ± standard deviation (n = 3).
524
525 **Fig. 8** Rate of nitrobenzoxadiazole-labeled triacylglycerol (NBD-TAG) production by AtPDAT1
526 reveals Michaelis-Menten kinetics to increasing NBD-diacylglycerol (NBD-DAG) and 16:0,18:1-DAG
527 concentrations (R^2 = 0.997 and R^2 = 0.975, respectively). Plots were generated using GraphPad Prism
528 8. The final concentration of NBD-DAG or 16:0,18:1-DAG in reactions was increased from 10 μM to
529 60 μM. The final concentration of 18:1,18:1-PtdCho or 16:0,[^{14}C]18:1-PtdCho was kept at 25 μM in all
530 reactions. Reactions were carried out at 30ºC for 60 min. Values represent mean ± standard deviation
531 (n = 3).
532
533 **Fig. 9** The effects of different solvents on fluorescence-based PDAT assays. Ethanol, diethyl ether or
534 benzene was used as solvents for the addition of substrates to microsomal fractions. Student's t-tests
535 indicate that diethyl ether and benzene are equivalent in terms of NBD-TAG production, and both
536 solvents are significantly superior to ethanol in terms of triacylglycerol production ($p<0.05$). All
537 reactions were carried out with 1.5 nmol NBD-DAG, 2.5 nmol 18:1,18:1-PtdCho, 100 μl of phosphate
538 buffer (pH 7.2) at 30ºC for 60 min. Values represent mean ± standard deviation (n = 3).
539

540

541

542

543 **Fig. 1** Schematic representation of the enzymatic reaction catalyzed by phospholipid:diacylglycerol

544 acyltransferase (PDAT). PDAT catalyzes the transfer of an acyl chain from the *sn*-2 position of

545 phospholipid to the *sn*-3 position of DAG. PL, phospholipid; DAG, diacylglycerol; LPL,

546 lysophospholipid; TAG, triacylglycerol; FA, fatty acid

547

548

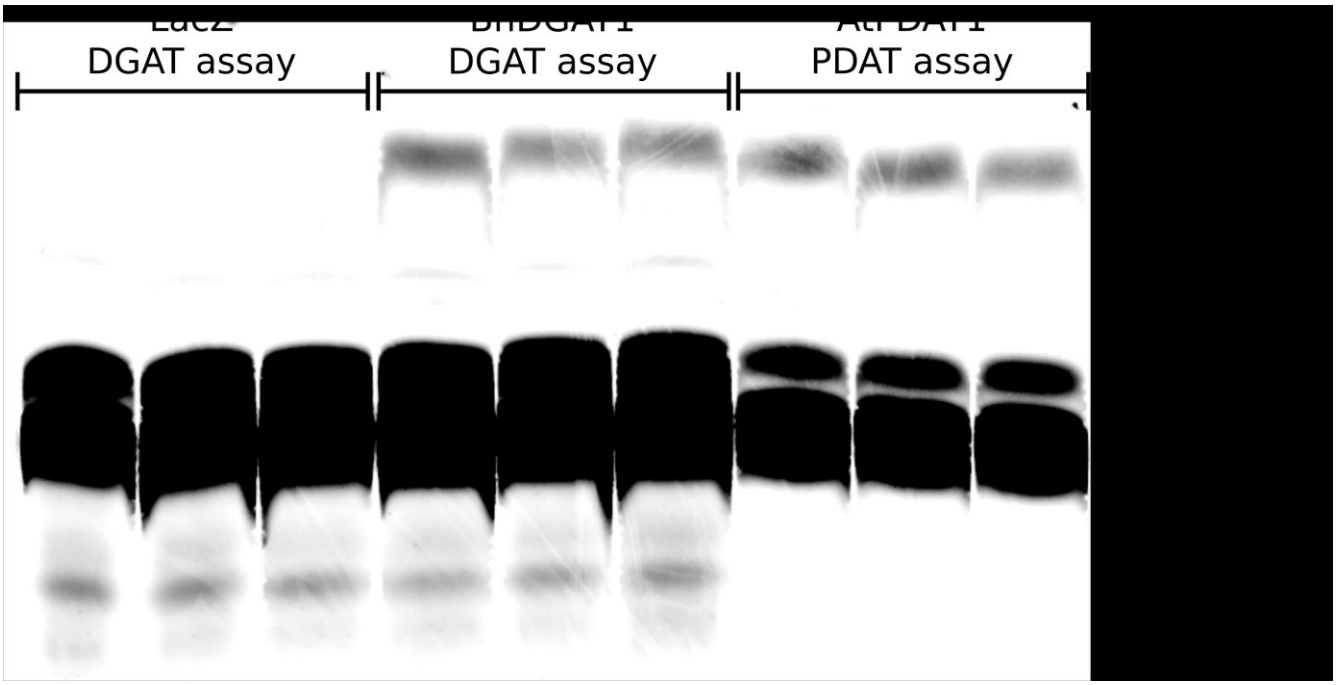

549

550 **Fig. 2** A representative TLC plate displaying results of enzymatic assays using fluorescence-labeled
551 substrate. Microsomal preparations from the *S. cerevisiae* quadruple mutant H1246 transformed with
552 either AtPDAT1 and BnDGAT1 were used as enzymes in the PDAT and DGAT assays, respectively.
553 For DGAT assay, fluorescent 1-palmitoyl-2-dodecanoyl-NBD-*sn*-glycero-3-glycerol (NBD-DAG) and
554 oleoyl-CoA were used as substrates. NBD-DAG spots are composed of 1,2-NBD-DAG (lower band)
555 and 1,3-NBD-DAG (upper band). Microsomes derived from yeast cells transformed with the *LacZ*
556 gene were used as the negative control. Following enzymatic assays, lipid fractions were extracted and
557 separated on TLC plates. NBD-TAG, NBD-labeled triacylglycerol. AtPDAT1, *Arabidopsis thaliana*
558 phospholipid:diacylglycerol acyltransferase 1; BnDGAT1, *Brassica napus* acyl-CoA:diacylglycerol
559 acyltransferase 1

560

561 **A**

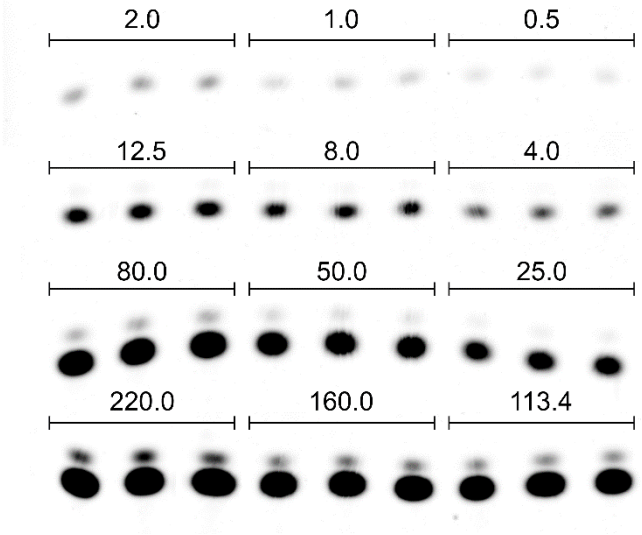

562

563 **B**

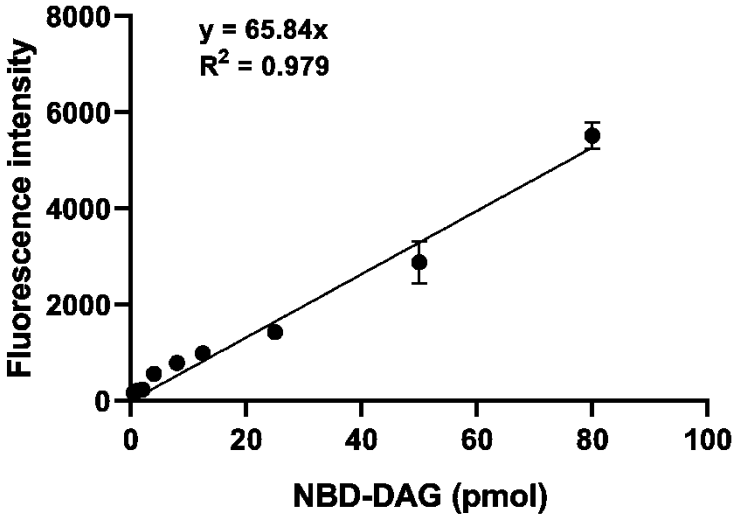

564

565 **Fig. 3** Establishment of a standard curve for the quantification of phospholipid:diacylglycerol
566 acyltransferase (PDAT) activity. (A) Scanned image of a representative TLC plate showing the
567 fluorescence intensity of 1-palmitoyl-2-dodecanoyl-NBD-*sn*-glycero-3-glycerol (NBD-DAG) in a
568 series of molar concentrations. (B) Standard curve for the quantification of NBD-labeled molecular
569 NBD-DAG or NBD-triacylglycerol (NBD-TAG). The linear range varies from 0.5 pmol to 80 pmol of
570 NBD-DAG.

571

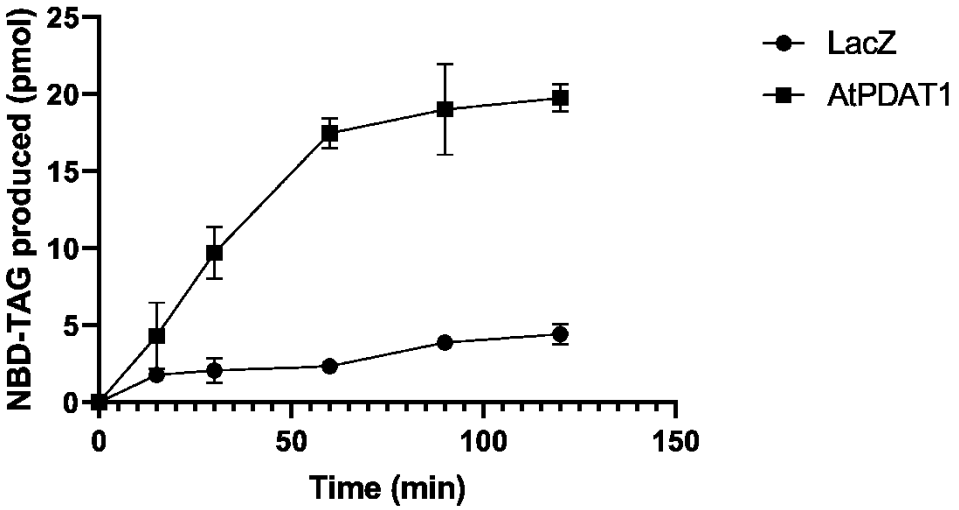

572

573 **Fig. 4** Time course curve of PDAT enzymatic reactions. Nitrobenzoxadiazole-labeled triacylglycerol
574 (NBD-TAG) produced from NBD-diacylglycerol (NBD-DAG) over time in the presence of
575 microsomal fractions from yeast heterologously expressing *Arabidopsis thaliana*
576 phospholipid:diacylglycerol acyltransferase 1 (AtPDAT1). Microsomes derived from yeast cells
577 transformed with the *LacZ* gene were used as a negative control. The reactions were catalyzed using 40
578 µg of microsomal protein in each case. All reactions were carried out with 1.5 nmol NBD-DAG, 2.5
579 nmol 18:1,18:1-PtdCho, 100 µl of phosphate buffer (pH 7.2) at 30ºC. NBD-TAG production increases
580 linearly up to 60 min (R^2 = 0.995). Values represent mean ± standard deviation (n = 3).

581

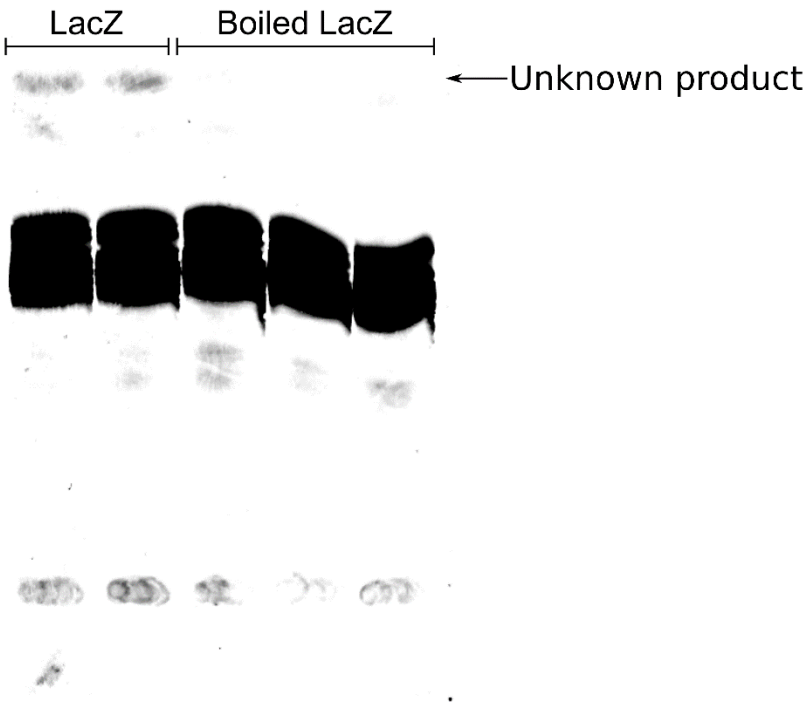

582

583 **Fig. 5** Production of unknown product with a similar migration distance to nitrobenzoxadiazole-labeled
584 triacylglycerol (NBD-TAG). The compound is not present in the boiled microsomal fractions from
585 yeast transformed with *LacZ*, which suggests an enzyme-catalyzed reaction. The reactions were carried
586 out using 40 µg of microsomal protein in each case. All reactions were added 1.5 nmol NBD-DAG, 2.5
587 nmol 18:1,18:1-PtdCho, and 100 µl of phosphate buffer (pH 7.2) and incubated at 30ºC for 60 min.

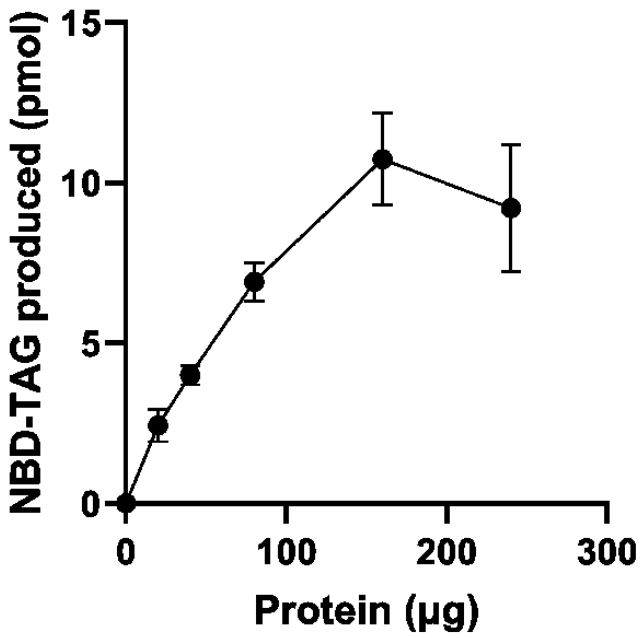

588

589 **Fig. 6** Production of nitrobenzoxadiazole-labeled triacylglycerol (NBD-TAG) in an enzymatic reaction
590 catalyzed by *Arabidopsis thaliana* phospholipid:diacylglycerol acyltransferase 1 (AtPDAT1) at
591 different concentrations. Microsomes derived from yeast cells transformed with the *LacZ* gene were
592 used as the negative control and weak fluorescent signals generated were subtracted from the
593 corresponding AtPDAT1 reactions as background. Microsome protein contents varied from 0 to 240 µg
594 in the reactions. All reactions were carried out with 1.5 nmol NBD-DAG, 2.5 nmol 18:1,18:1-PtdCho,
595 100 µl of phosphate buffer (pH 7.2) at 30ºC for 60 min. Values represent mean ± standard deviation (n
596 = 3).

597

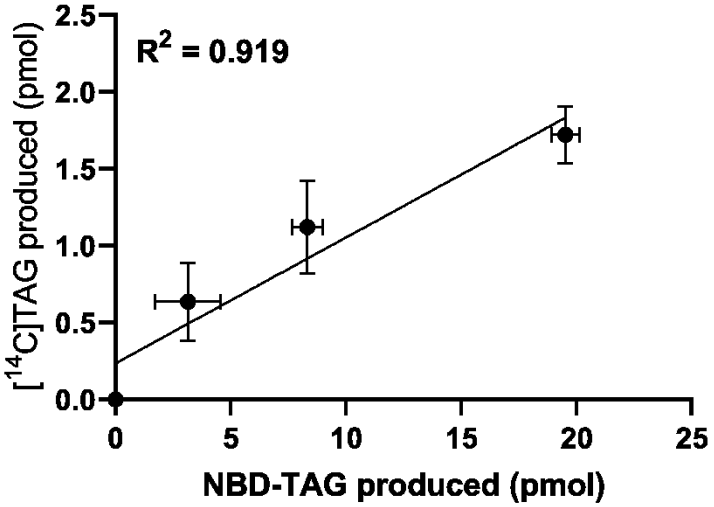

598

599 **Fig. 7** Comparison between the fluorescence-based PDAT assay and the conventional assay with
600 radiolabeled chemicals for a wide range of microsomal protein amounts (0, 20, 40, and 80 μg)
601 containing *Arabidopsis thaliana* phospholipid:diacylglycerol acyltransferase 1 (AtPDAT1) shows a
602 good correlation (R^2 = 0.919). To avoid the influence of endogenous PtdCho on the conventional assay,
603 the amount of protein was kept constant at 80 μg by mixing microsomes derived from yeast cells
604 transformed with the *AtPDAT1* and *LacZ* genes. The conventional assay reactions were carried out with
605 2.5 nmol 16:0,[^{14}C]18:1-PtdCho, 1.5 nmol 16:0,18:1-DAG, 100 μl of phosphate buffer (pH 7.2) at 30ºC
606 for 60min. Values represent mean ± standard deviation (n = 3).

607

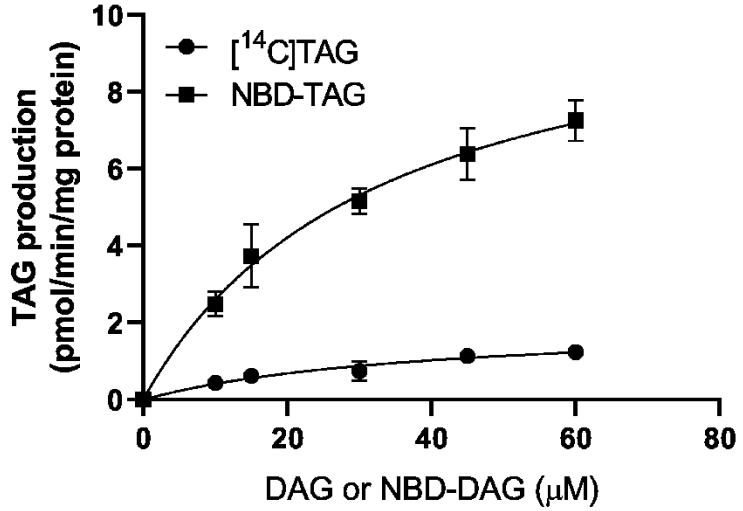

608

609 **Fig. 8** Rate of nitrobenzoxadiazole-labeled triacylglycerol (NBD-TAG) production by AtPDAT1

610 reveals Michaelis-Menten kinetics to increasing NBD-diacylglycerol (NBD-DAG) and 16:0,18:1-DAG

611 concentrations ($R^2 = 0.997$ and $R^2 = 0.975$, respectively). Plots were generated using GraphPad Prism

612 8. The final concentration of NBD-DAG or 16:0,18:1-DAG in reactions was increased from 10 μM to

613 60 μM. The final concentration of 18:1,18:1-PtdCho or 16:0,[^{14}C]18:1-PtdCho was kept at 25 μM in all

614 reactions. Reactions were carried out at 30ºC for 60 min. Values represent mean ± standard deviation

615 (n = 3).

616

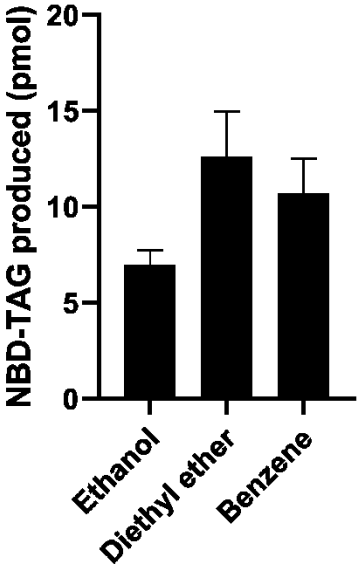

617

618 **Fig. 9** The effects of different solvents on fluorescence-based PDAT assays. Ethanol, diethyl ether or
619 benzene was used as solvents for the addition of substrates to microsomal fractions. Student's t-tests
620 indicate that diethyl ether and benzene are equivalent in terms of NBD-TAG production, and both
621 solvents are significantly superior to ethanol in terms of triacylglycerol production ($p<0.05$). All
622 reactions were carried out with 1.5 nmol NBD-DAG, 2.5 nmol 18:1,18:1-PtdCho, 100 µl of phosphate
623 buffer (pH 7.2) at 30ºC for 60 min. Values represent mean ± standard deviation (n = 3).

624